Available online at www.CivileJournal.org

Civil Engineering Journal

(E-ISSN: 2476-3055; ISSN: 2676-6957)

Vol. 8, No. 06, June, 2022

Slenderness in Steel Fibre Reinforced Concrete Long Beams

Ravpreet Kaur [1, 2*], Harvinder Singh [3]

[1] *Research Scholar, Department of Civil Engineering, IKG Punjab Technical University, Punjab, India.*

[2] *Assistant Professor, Department of Civil Engineering, SGT University, Haryana, India.*

[3] *Professor, Department of Civil Engineering, GNDEC, Ludhiana, Punjab, India.*

Received 18 March 2022; Revised 23 May 2022; Accepted 29 May 2022; Published 01 June 2022

Abstract

Slenderness influences in steel fibre reinforced concrete (SFRC) long beams are not adequately addressed in current concrete design regulations. The present guidelines are confined to semi-empirical formulations for limiting slenderness ratio, but largely restricted to RC beams. Many scholars have already examined RC long beams and successfully presented the slenderness ratio formula for RC long beams. This article proposes a novel term for limiting the slenderness ratio for SFRC long rectangular beams based on the fundamental principle of mechanics and taking into account the slenderness impact of RC long beams as well as the flexural moment capacity of SFRC beams. The suggested formulation for limiting slenderness ratio agrees closely with experimental data and may reliably forecast the mode of collapse. The proposed limiting slenderness ratio formulation takes into consideration beam end circumstances, loading conditions, concrete strengths, steel, tension and compression reinforcement ratios, and transverse reinforcement ratios, among other factors. It is revealed that a wide variety of slenderness limits may be achieved for varied sets of design parameters. The researchers' predictions and the suggested equation are compared to the test results of 9 SFRC beams. The suggested equation fits well with the results of the tests that have been done so far.

Keywords: SFRC; Steel Fibres; Slenderness; Long; Hooked End.

1. Introduction

Slenderness impacts in RC beams are restricted to normal span beams as per the Indian building design code [1]. However, long beams (RC) exhibit a distinctive response because of slenderness from those of regular sized/span beams. The collapse mechanism of unusually long beams is found to be sudden destabilization. A relatively thick beam would be vulnerable to the effects of slenderness and would fail in flexure at a load corresponding to the moment smaller than the flexural moment capacity, implying material failure. But owing to the research on long beams in the past few decades, it has been learnt that the design standards [1-5] stipulated for slenderness in normal span beams cannot predict the behaviour of these RC long beams accurately, and investigations have further demonstrated that the slenderness of these reinforced concrete long beams is also dependent on different design factors. It has been learnt that the slenderness depends upon the values of M_{uf} (ultimate flexure moment capacity) and M_{bcr} (critical buckling moment), so proper estimation of both (M_{bcr} and M_{uf}) is required to precisely predict the behaviour of these beams. Currently, there is no approach in the design codes for evaluating M_{bcr} for RC long beams and M_{uf} for SFRC long beams in BIS design codes. In recent years, many researchers have analysed the RC long beams and have quite accurately predicted the behaviour of these RC long beams and, hence, forth put forward a mathematical model for calculating the critical buckling moment and the slenderness [6-8].

* Corresponding author: ranjodh6051@gmail.com

http://dx.doi.org/10.28991/CEJ-2022-08-06-011

Revathi & Menon [6, 7] investigated the extremely and relatively moderate long RC beams and developed as well as presented mathematical equations to compute M_{bcr} for these rectangular beams. It was asserted that a number of sets of design parameters can have a broad range of slenderness limits and further presented a limiting value of slenderness ratio (λ) by comparing the critical buckling moment, M_{bcr} with the ultimate flexural moment capacity, M_{uf} in the mathematical expression:

$$\lambda = \frac{C_1}{10C_2} \cdot \frac{E_c}{R} \cdot \sqrt{\alpha\beta} \quad (1)$$

where C_1 and C_2 are variables that corresponding to the support conditions of beam and the applied loading, respectively.

The '*flexural resistance factor*' R for a beam section of width b and having an effective depth d) is $R = M_{uf} / (bd^2)$; and α, β are the 'effective flexural rigidity' and 'torsional rigidity coefficients' that are a function of fracturing and and tension stiffening, respectively. The suggested formula for M_{bcr} was verified using seven tests performed by Revathi & Menon [6], three tests devised by Sant & Bletzacker [9], and eleven tests designed by Massey [10]. As many as eight beams that Revathi & Menon [7] tested collapsed by buckling actually failed in the flexural tension mode, despite the fact that the flexural capacity in majority of these cases was lowered due to slenderness as stated by Girija & Menon [8]. Girija & Menon [8], further conducted 15 laboratory tests on slender RC beams rectangular in shape, and hence modified the formula for critical buckling moment as presented by Revathi & Menon [7] as it further took into account the non-linear behaviour of concrete leading to development of cracks.In addition to this, an improved version of mathematical expression presented by Revathi & Menon [7], was suggested by Girija & Menon [8] for calculating the slenderness ratio $\lambda = \sqrt{M_{uf}/M_{bcr}}$, which gave much more accurate results.

The current research study is performed on steel fibre reinforced concrete long beams, as owing to the reduced ductile tolerance of concrete, the reinforced concrete loses its tensile strength and fails in a fragile manner [11], so by adding steel fibres, as volume reinforcement, not only can resist shear but also overcomes the flaws in concrete, by reducing and deferring the crack propagation and improving the complete performance of reinforced concrete structural system [11]. Concrete when strengthened with discontinuous, small, and dispersed fibres is considered to be a composite material with high fracture resistance due to the fibres' capacity to transmit tensile loads across crack surfaces (crack-bridging). The past studies on steel fibres have affirmed that the steel fibres have traditionally been known to increase the strength in bending, in tension and show a better fracture response as well as the energy absorption capacity. The researchers have indeed been investigating their efficacy on the flexural behaviour of these reinforced concrete structural elements for several years now. The steel fibrous concrete (SFC) shows improved cracking behaviour, decreased fracture size, limited crack growth, and prolonged concrete failure which further improves the flexural fracture resistance when reinforced with standard steel rebars [12-14]. Deformed or hooked-ended steel fibres with larger l/d ratio have also been shown to successfully enhance fracture resilience, energy loss, and ductility indices [15, 16]. The mathematical study of concrete structural sections reinforced with steel rebars and fibres, the incorporation of workable fundamental stress–strain relation of steel fibre reinforced concrete under compression as well as tension offers logical, reasonable and precise forecasting of the flexural evaluation in context of bending stress curves versus analytical curves [17].

It is due to the lack of adequate predictive techniques for determining the true behaviour of concrete and steel fibres in shear strength. Considering the absence of construction standards and regulations, a number of researchers conducted experiments and presented mathematical equations for predicting the shear strength of SFRC beams [18-25]. The hypothesis, on the alternative hand, accords strongly with the lab tests from that which it is developed, yet it does not agree well with the other test findings. As a result, mathematical models for predicting the flexural strength of SFRC beams using a wide range of experimental data are needed, taking into account the real contribution of steel fibres and concrete, as well as their interactions. The formula for ultimate flexural moment, $M_{uf}(=RBd^2)$ as in Indian standard codes (IS 456:2000) can be very well applied to RC long beams but not to the SFRC long beams as it is silent on effect of adding the fibres to the RC and thus cannot estimate the M_{uf} for SFRC beams. However the formula for calculating the ultimate flexural moment capacity of SFRC beams as proposed by Singh [26] suffices with lab tests. Since there are no such formulae or mathematical model for the slenderness limits and hence accurately predict the behaviour of SFRC long beams, the present study aims to present an analytical equation for predicting the slenderness limits of these beams. For long beams, different formulae to calculate critical buckling moment were proposed but the one suggested by Girija & Menon [8] defied the flaws and accounted for the non-linearity and cracking behaviour of concrete. When compared lab test results of SFRC long beams performed in this study, the suggested formulae for slenderness presented here accurately predict the slenderness limit and hence the mode of failure of these SFRC long beams as the construction sector is interested primarily in the possible and effective utilization of steel fibres. This would offer engineers and consultants with a guideline for the deciding the span of long SFRC beams quantity of fibre and aspect ratio of steel fibres in the design of SFRC long beams. As a result, this precise analytical model for predicting the slenderness limit of SFRC long beams will be used in order to establish design recommendations or regulations that would inevitably make SFRC long beams adaptive where-ever suitable in common construction.

2. Research Significance

Slenderness can have an undesirable impact on the performance of RC beam by developing a rapid imbalance failure or a significant reduction in flexural strength. Numerous studies in past provided theoretical models to predict slenderness limit for RC long beams based on their test findings, but none for SFRC long beams. The formula $\lambda = \sqrt{M_{uf}/M_{bcr}}$ presented by Girija & Menon [8], however accurately estimate the slenderness in rectangular RC beams. Since, these models could not account for the combined influence of steel fibres and other variables in forecasting slenderness limits for SFRC long beams with conventional reinforcement. So a semi-empirical formulation for estimating the slenderness limits (Ld/b^2) for SFRC long beams is provided in this study. The methodology followed in this research study is shown in the flowchart in Figure 1.

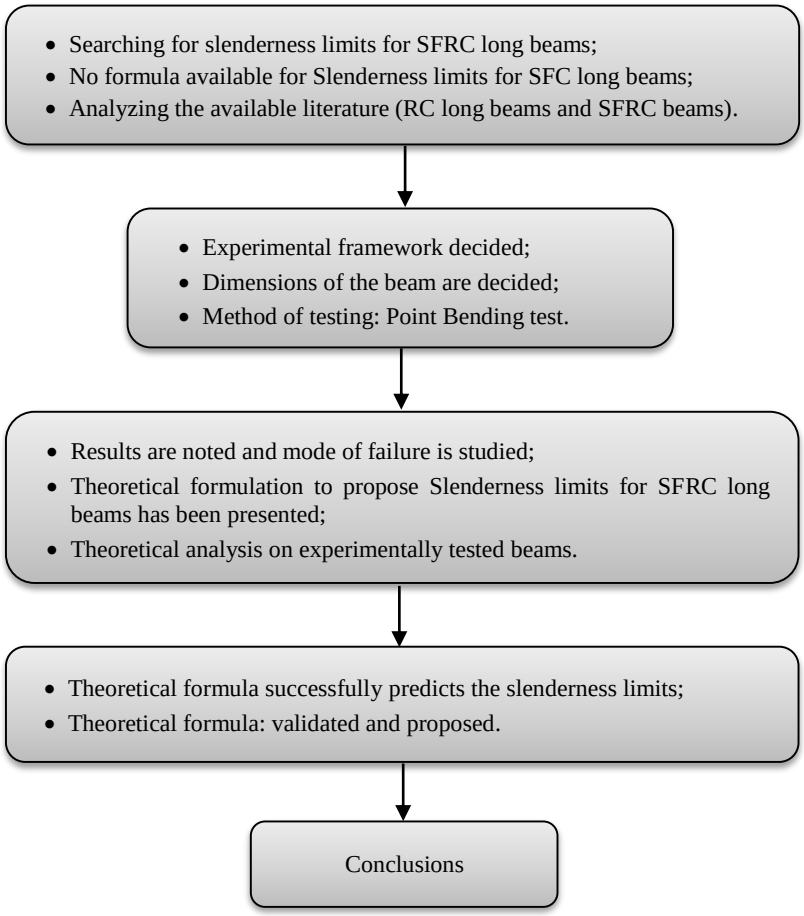

Figure 1. Flowchart showing the methodology followed in the research

3. Experimentation Method

The study was carried out at the Heavy Testing Laboratory at GNDEC, Ludhiana. A total of 9 under-reinforced rectangular beams were casted and tested. The size of beams were decided on the basis of the limiting slenderness ratio for RC long beams established previously by Revathi & Menon [7]. The beams, were 80mm in width and 360mm depth and span of 5m, were casted. The casting was carried out in three separate batches for three different concrete grades; M1 ranging from 31-36 N/mm^2, M2 ranging from 42-44 N/mm^2, M3 ranging from 55-59 N/mm^2. For each grade of concrete, one control beam (that does not include steel fibres) was casted. The remaining samples, on the other hand, were casted with 1% volume fraction of steel fibres. Additionally, to study the effect of aspect ratio of steel fibres on the behavior of these SFRC long beams, 2 different aspect ratios (63.63 and 77.78 of hooked end steel fibres) were considered for this investigation. The beam ends were simply supported in the vertical and lateral planes, but were torsionally restrained and allowed to twist. Four point bending test was performed and the experimental arrangement (as shown in Figure 2) was based on Hansell & Winter's [27] study, and it remained explicitly the same as the one used by previous studies. It comprised of two load assemblies built up using rollers in between two steel plates to convey the applied point loads with little constraints laterally. Preliminary test was performed with the load setup to guarantee that the imposed loading only marginally restrains the beam's lateral deflection.

Figure 2. Test Setup for experimental study

3.1. Specimens

Table 1 lists the beam size and reinforcing specifications of the test samples. The tension reinforcement in all the test samples was kept same throughout at 1.09%.The initial imperfection of 1-6 mm was recorded in all beams. The change in parameters was accomplished in the 9 beams by changing the f_{ck} for concrete and aspect ratio of steel fibres.

Table 1. Test beam Data

S. No.	Beam Label	Dimensions b × D × L (mm)	Fibre type	Aspect Ratio	Average cube strength (MPa)	Initial Imperfection (mm)	Remarks
1	M1S0	80×360×5000	-	-	31.00	4	Control beam (without fibres-grade 1)
2	M1S1P1	80×360×5000	Hooked-end	63.63	33.40	1	SFRC beam with Grade M1
3	M1S2P1	80×360×5000	Hooked end	77.78	34.20	3	SFRC beam with Grade M1
4	M2S0	80×360×5000	-	-	42.20	3	Control beam (without fibres-Grade M2)
5	M2S1P1	80×360×5000	Hooked-end	63.63	43.00	1	SFRC beam with Grade M2
6	M2S2P1	80×360×5000	Hooked end	77.78	42.00	1	SFRC beam with Grade M2
7	M3S0	80×360×5000	-	-	55.0	3	Control beam (without fibres-Grade M3)
8	M3S1P1	80×360×5000	Hooked-end	63.63	57.4	4	SFRC beam with Grade M3
9	M3S2P1	80×360×5000	Hooked end	77.78	58.9	3	SFRC beam with Grade M3

3.2. Materials

Fine aggregate was Zone II with fineness modulus 4.96 and specific gravity 2.6, (the grading curve for fine aggregates is shown in Figure 3) while coarse aggregate was crushed granite stone with a maximum size of 16 mm and fineness modulus of 1.98and specific gravity as 2.97 (the grading curve for coarse aggregates is shown in Figure 4). The weight ratio of the mix for M1 was 1:2.16:2.66: with w/c ratio as 0.47 and admixture as 0.4%, for M2, it was 1:1.62:2.24 with w/c ratio as 0.39 and admixture as 0.42%. Both grades M1 and M2 use PPC. While mix design for high grade concrete, M3 was 1:1.37:2.84 with w/c ratio as 0.34 and admixture as 0.5%, fly-ash as 0.18% and silica fumes as 0.0625% with OPC43 grade. The longitudinal reinforcing bars of diameter 10 mm were made of steel with a characteristic yield stress of 500 MPa, while the stirrups were 6mm in diameter and made of steel with a characteristic yield stress of 250 MPa. During each casting, three cubes were casted and the mean cube strength values were found out from the peak load on compression testing machine and 2 cylindrical specimens were casted for finding the split tensile strength. These values of compressive strength and split tensile strength were utilized in the beam specimen strength computations.

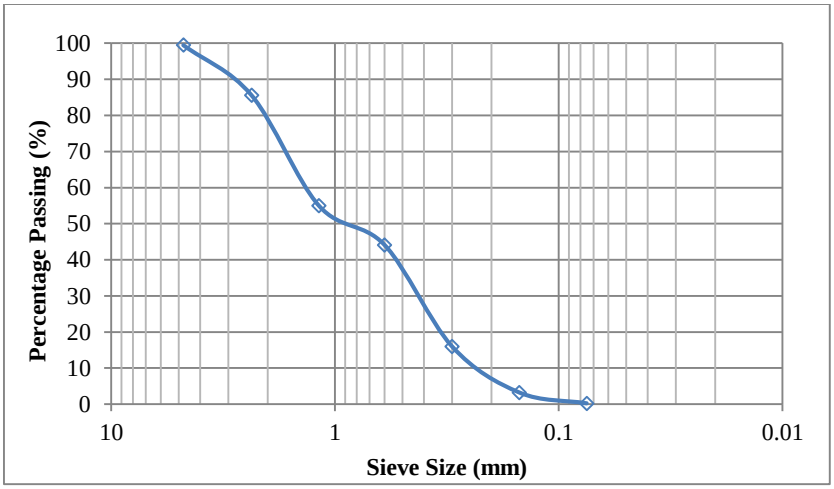

Figure 3. The grading curve for fine aggregates

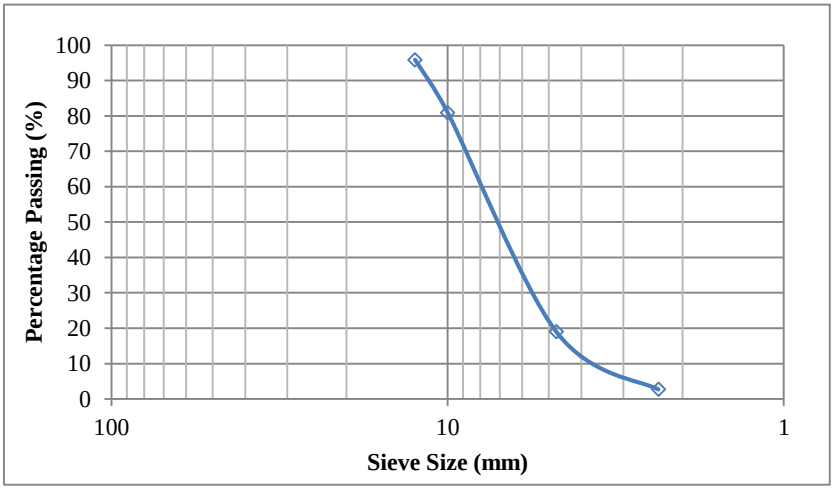

Figure 4. The grading curve for coarse aggregates

3.3. Instrumentation for the Specimen and the Test Method

At mid-span, dial gauges with a precision of 0.01 mm were utilised to monitor the lateral and vertical deflections at the centre point of the effective span. It was ensured that the load was applied without any damage. All the beams were gradually loaded, with the predicted failure occurring after 15 to 20 load stages. As calculated from theoretical formulation, the beams were loaded to failure, and dial gauges were used to record a complete set of deflection values at each load increment. The peak load and mode of collapse were noted. Table 2 also shows the test beam failure loads and observed mode of failure during the laboratory investigation.

Table 2. Test results

S. No.	Beam	f_{ck}	E_c	Expt. peak load	Observed Failure
1	M1S0	31.00	27838.82	43.200	Flexural tension failure (with negligible lateral deflection)
2	M1P1S1	33.40	28896.37	48.500	Flexural failure with enhanced tensile capacity (with lateral deflection)
3	M1P1S2	34.20	29240.38	48.400	Flexural failure with enhanced tensile capacity (with lateral deflection)
4	M2S0	42.20	32480.76	52.500	Flexural failure with enhanced tensile capacity (with lateral deflection)
5	M2P1S1	43.00	32787.19	50.200	Flexural failure with enhanced tensile capacity (with lateral deflection)
6	M2P1S2	42.00	32403.70	52.900	Flexural failure with enhanced tensile capacity (with lateral deflection)
7	M3S0	55.0	37080.99	44.80	Flexural failure with enhanced tensile capacity (with lateral deflection)
8	M3P1S1	57.4	37881.39	50.80	Failure due to instability (i.e. large lateral deflections)
9	M3P1S2	58.9	38373.17	46.20	Failure due to instability (i.e. large lateral deflections

The results indicate that the suggested expressions for M_{bcr} and limiting slenderness ratio for slender RC beams, suggested by Girija & Menon [8] holds true since the 4 point bending test performed in laboratory on the specimens of 3 control beams show comparable results and, hence the formulation published by Girija & Menon [8] can be further

applied for deriving the formulae for flexural moment capacity and limiting slenderness ratio for steel fibre reinforced concrete long beams and the formulation must be validated against all above laboratory tests performed on the specimens of SFRC long beams as in Table 2.

3.4. Observed Mode of Failure

Case 1: Flexural tension failure (with negligible lateral deflection)

When the cracks appear due to flexural failure, lateral deflection is zero or it's actually negligible generally observed in the soffit area extending gradually to both the sides under the application of load. These cracks propagate upwards thus leading to final collapse due to concrete crushing in the compression zone with prior warning.

Case 2: Flexural failure with enhanced tensile capacity (with lateral deflection)

When the flexural cracks appear due to application of load with controlled lateral deflection .The cracks generally observed in the soffit area extending gradually to both the sides under the increased loading. These cracks propagate upwards similar to Case 1 but in this case the beam can take load compared to the calculated capacity thus leading to final collapse due to increased vertical deflection due to bending with prior warning.

Case 3: Failure due to instability (i.e. large lateral deflections)

Where the beam is not able to carry any load further due to large lateral deflection or increased twisting with loading and cracks, the failure occurs suddenly as the beam moves out of the load assembly due to large lateral deflection and the failure occurred at a load value less than the calculated flexural load capacity of the beam.

3.5. Load vs. Deflection Curves

The load-deflection curves from Figures 5 to 7 show how with variation in concrete grade and Figures 8 and 9 shows how the aspect ratio of steel fibres impacts the load carrying capacity and deflection control in the test beams. Comparison of Load deflection curve from Experimental study for Grade M1, M2 and M3 (Figures 5 to 7).

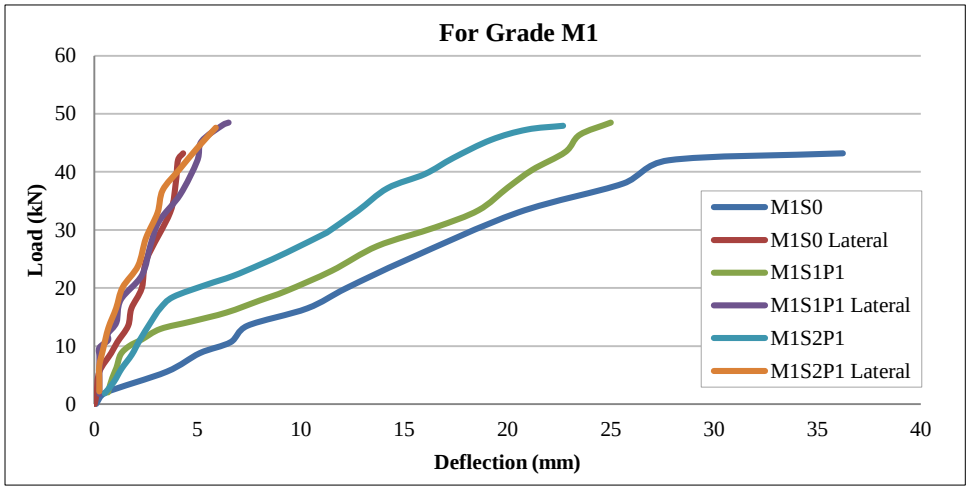

Figure 5. Comparison of Load deflection curves for Grade M1

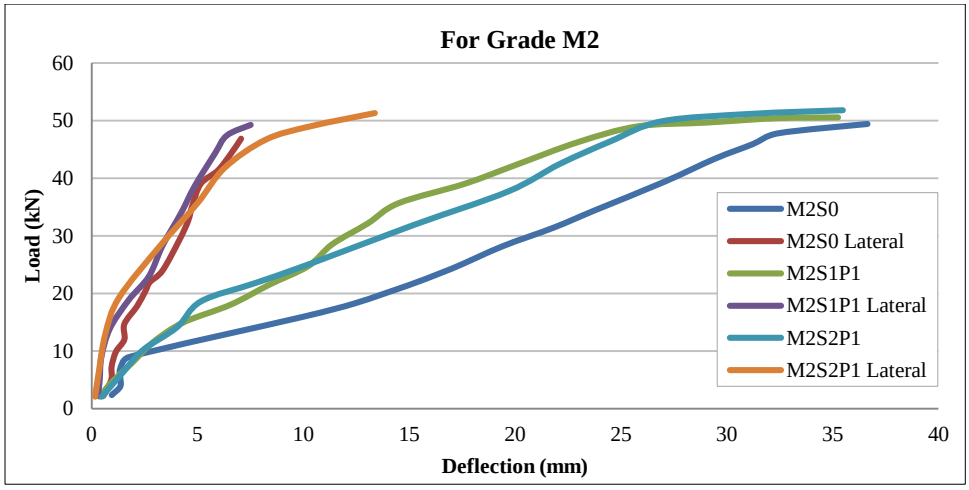

Figure 6. Comparison of Load deflection curve for Grade M2

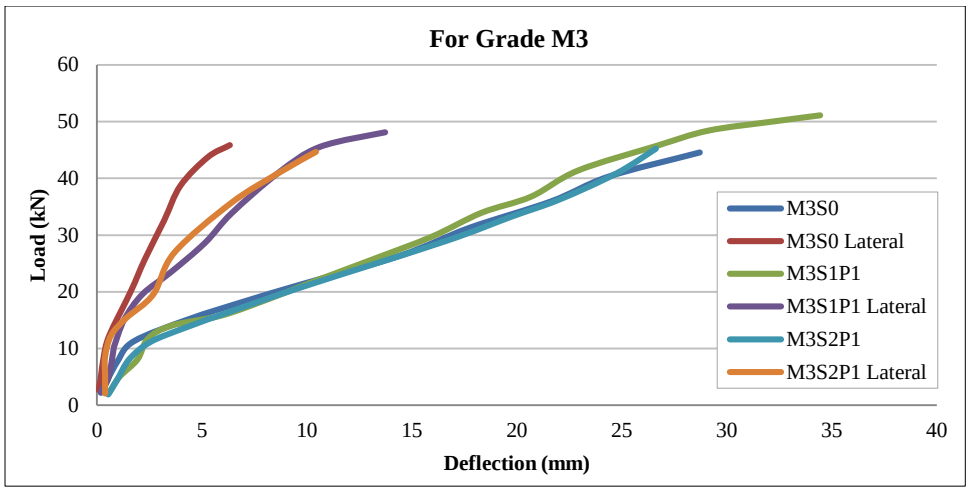

Figure 7. Comparison of Load deflection curve for Grade M3

Comparison of Load deflection curve for Fibre type S1 and S2 (Figure 8 and 9).

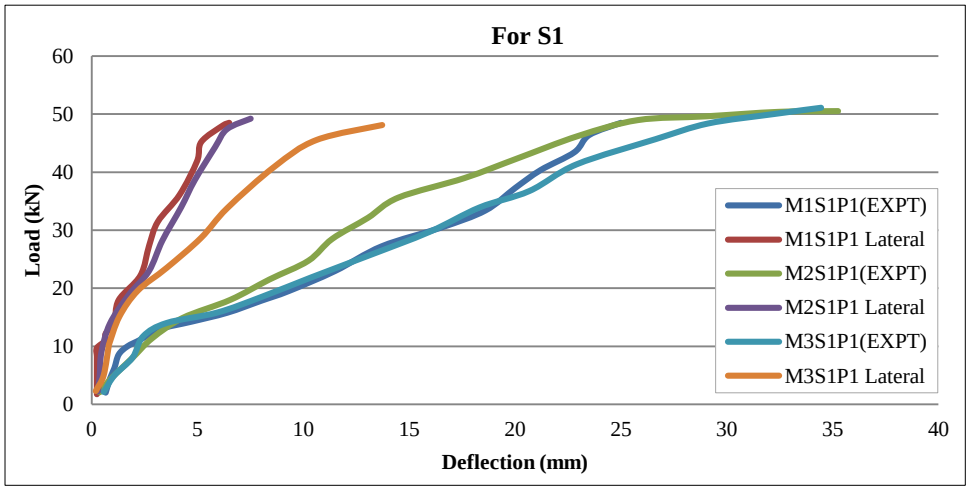

Figure 8. Comparison of Load deflection curve for Fibre type S1

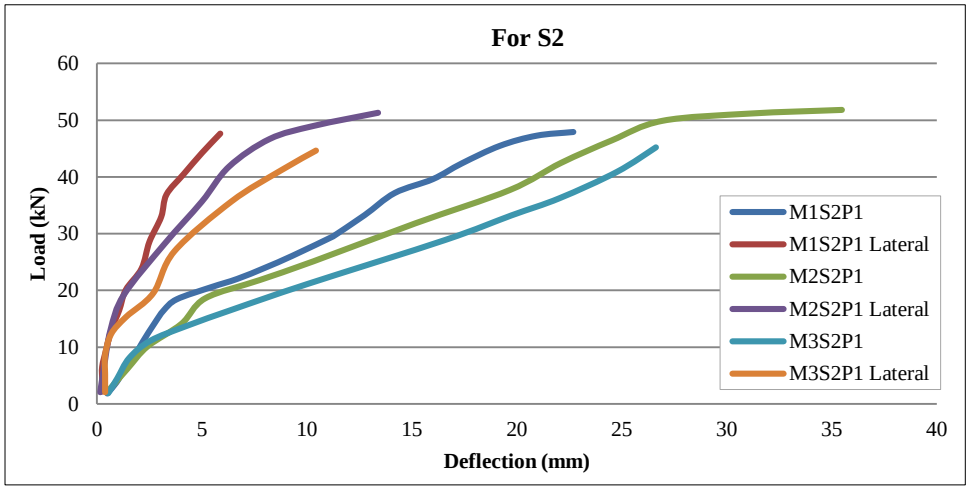

Figure 9. Comparison of Load deflection curve for Fibre type S2

4. Theoretical Formulation

4.1. Critical Buckling Moment

The first step is to compute the critical buckling moment.

From the previously published studies, it has been learnt that for a rectangular section, critical buckling moment is derived from the fundamental concept of considering potential energy as constant [28]. On the application of load, the

deformation takes place in both vertical direction (in y direction) as well as in the horizontal direction (in x direction) along with twisting (x-y direction) of the deformed section (Figure 10 shows the experimental procedure and Figure 11 shows the deflection in the beam).

Figure 10. Horizontal deflection in Slender RC beam with the application of load as captured during experimental testing

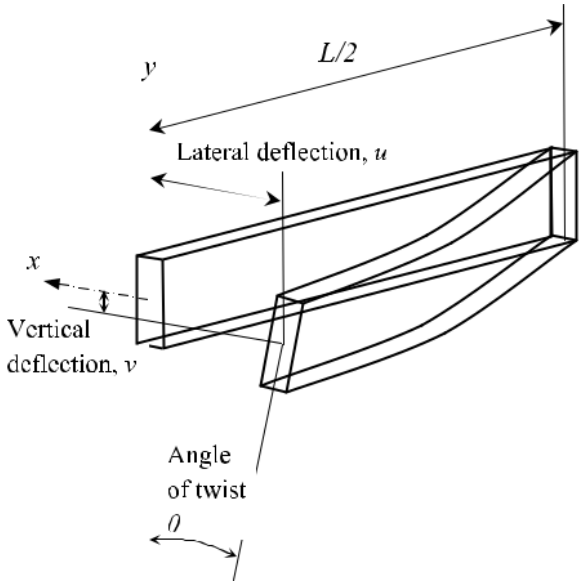

Figure 11. The cross section of mid span of slender beam in laterally deflected position [8]

$$\delta \prod = \delta U + \delta V = 0 \quad (2)$$

where $\delta\prod$, δU, and δV represent the initial change in total potential energy ($\prod$), strain energy (U) owing to horizontal bending and twisting, and loading potential (V) for the simply supported structural member subjected to proportioned middle third loading, correspondingly.

The in-plane deformation component can be eliminated while evaluating displacement as it de-links the in-plane action from the failure in the horizontal direction [8, 29]. For thin rectangular components, the impact of twisting can be ignored [30], resulting in captured strain energy and load capacity in horizontal twisting bending. The stored potential energy and load stored in horizontal twisting bending can be written as:

$$U = \frac{1}{2}\int_0^L [EI_y(u")^2 + GJ(\theta')^2]dz \quad (3)$$

$$V = \int_0^L M_x \theta u" dz - \frac{a}{2}\int_0^L P\theta^2 \, dz \quad (4)$$

where u is the sideways deflection, θ is the measure of twisting angle, P is the entire load transmitted, a is the distance of load applied above the shear centre (Figure 12) and M_x is the bending moment owing to the load application about the principal bending axes.

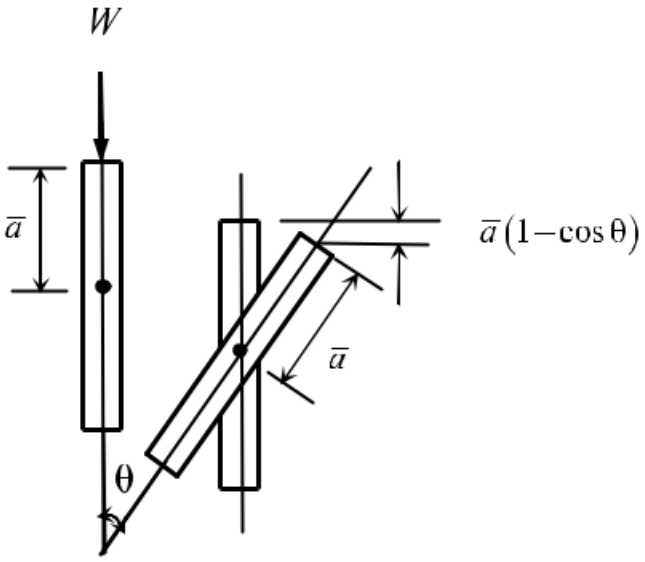

Figure 12. The load applied above shear center [8]

The expression of M_{bcr} reduces to the below equation:

$$M_{bcr} = 1.09\frac{\pi}{L}\sqrt{EI_y GJ} \times \left(\sqrt{1+\left(1.57\frac{a}{L}\sqrt{\frac{EI_y}{GJ}}\right)^2} - 1.57\frac{a}{L}\sqrt{\frac{EI_y}{GJ}}\right) \quad (5)$$

where EI_y is the sideways flexural rigidity and GJ is the torsional rigidity.

The above formulation, for thin beams with simply supported ends, rectangular cross sections loaded at the central third points and casted of homogenous elastic substance could not be easily applied to RC members, since it accounts for cracking and non-linearity of concrete. Beacuse of which Revathi and Menon [6, 7] developed formulas for effective bending and torsional resistance for fractured concrete beams.

4.1.1. Effective Flexural Stiffness

To obtain the effective stiffness in flexure for any value of load, the relationship between moment and curvature (M–ϕ) of RC beams as presented by Bazant & Oh [31] applied in this study (Figure 13). Although Branson's model [32] is only applicable to service loads, the framework hence is curated from basic material properties which can predict bending and deflections up to the ultimate load. This moment curvature relationship is hence developed applying strain interaction, as proposed by Bazant & Oh [31].

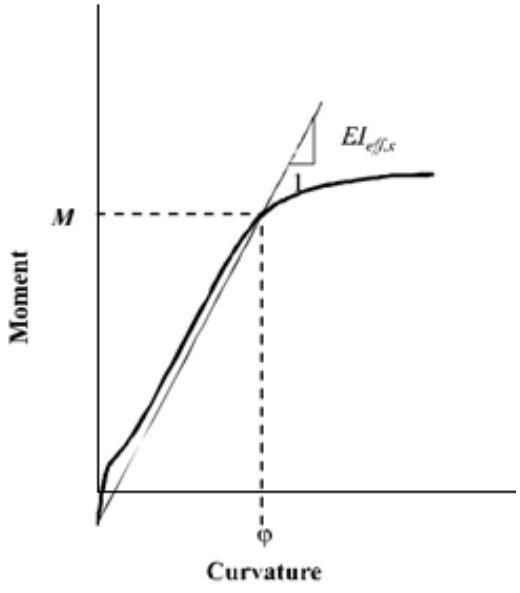

Figure 13. Typical moment (M)-curvature (φ) relationship [8]

The fraction, M/ϕ, corresponds to any point on this graph (for a given moment level) and is a measurement of effective flexural stiffness with respect to the primary axis, ($E\mathrm{I}_{\mathrm{eff,\,x}}$). The secant elastic modulus is obtained from the specified nonlinear stress vs. strain graph of concrete (Figure 14) which corresponds to the excessive fibre compression stress and strain.

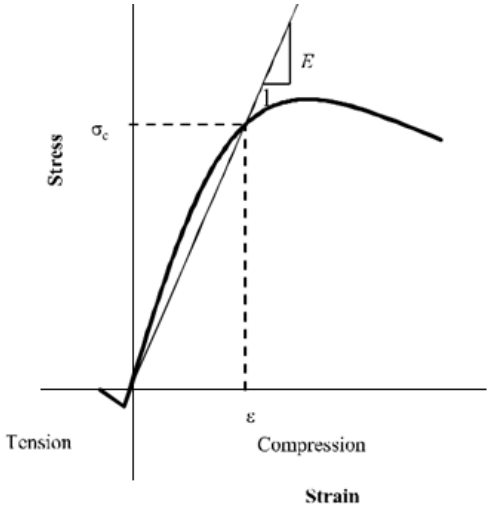

Figure 14. A typical Stress-strain curve of concrete [8]

The M–ϕ curve's effective moment of inertia ($\mathrm{I}_{\mathrm{eff,\,x}}$) accounting for the fracturing caused by primary axes bending as well as the non - linearity of concrete. This will have a negative impact on lateral flexural stiffness. This drop is supposed to be characterized by an analogous effective rectangular beams, with the same width b but a decreased depth d_{eqv}, leading to the estimated value of $\mathrm{I}_{\mathrm{eff,x}}$, at every moment level, M, whereby the calculated value of $\mathrm{I}_{\mathrm{eff,y}}$ may now be determined as well. For the constraint M = $\mathrm{M}_{\mathrm{bcr}}$, the converged values of $\mathrm{I}_{\mathrm{eff,\,x}}$, d_{eqv} and $\mathrm{I}_{\mathrm{eff,y}}$ may be produced via an iteration including repetitive applications of Equation 5.

For this crucial state, the value of effective horizontal flexural stiffness is represented by B_{eff}, which is stated as follows:

$$B_{eff} = E\mathrm{I}_{\mathrm{eff,\,y}} = E\left(\frac{d_{eqv}b^3}{12}\right) \tag{6}$$

4.1.2. Torsion Rigidity (Effective)

In this work, Tavio and Teng [33] provided the solution for effective twisting stiffness, K_{eff} of fractured concrete beams, which is a revised form of the expression published by Hsu [34]:

$$K_{eff} = \frac{4\mu E_S {A_o}^2 A_c}{{p_o}^2\left(\frac{1}{\rho_t}+\frac{1}{\rho_{tr}}\right)} \tag{7}$$

where μ is the rigidity multiplier often taken as 1.5 as suggested by Tavio & Teng [33], $\rho_t = A_l/A_{\mathrm{c}}$ and $\rho_{tr} = \frac{A_t p_1}{A_c s}$ denotes the ratio of reinforcement in both longitudinal and transverse directions respectively A_o, A_c and p_o are the cross-sectional properties of the section of the beam as shown in the Figure 15.

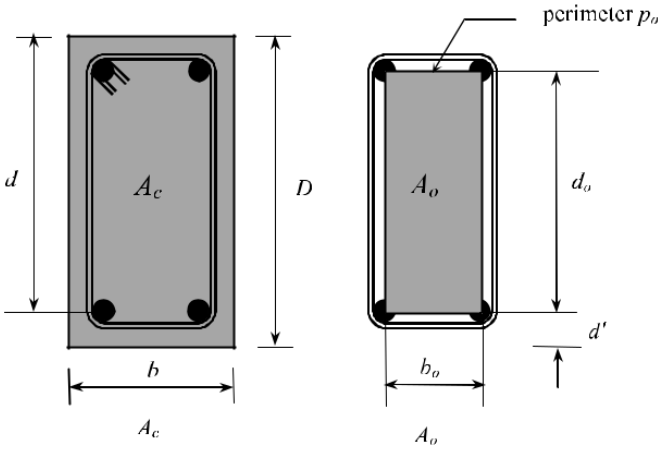

Figure 15. The cross section of the beam

4.1.3. Critical Buckling Moment for a RC Beam

The formula for M_{bcr} stated in Equation 5 (suitable for symmetric position of middle-third loading with ends being simply supported) may be represented as follows in contexts of effective lateral flexural rigidity (B_{eff}) and torsional rigidity (K_{eff}):

$$M_{bcr} = 1.09 \frac{\pi}{L}\sqrt{B_{eff}K_{eff}} \times \left(\sqrt{1+\left(1.57\frac{a}{L}\sqrt{\frac{B_{eff}}{K_{eff}}}\right)^2} - 1.57\frac{a}{L}\sqrt{\frac{B_{eff}}{K_{eff}}}\right) \quad (8)$$

It should be highlighted that the real estimation of M_{bcr} necessitates the use of an iterative operation because it is dependent on B_{eff} evaluation, Equation 6, which necessitates the use of gradual strain loading method to create the M– ϕ correlation previously stated.

The formula of M_{bcr} as in Equation 8 can be simplified further to general formula which can be applied to a number of loading conditions and boundary setups as given below:

$$M_{bcr} = \frac{C_1 C_3}{C_2 L}\sqrt{B_{eff}K_{eff}} \quad (9)$$

The above stated formulation for M_{bcr} has parameters which can be described as C_1 is for applied loading condition (which has a value of π for pure bending and 1.35π under the central concentrated load), and C_3 is a component that contributes for the end support. C_2 accounts for the beam's support conditions (a value of unity for beam with ends simply supported) and C_3 accounts for the position of loads with regards to the rectangular beam's centroidal axes (=1, when the load is applied at the centroid) [30].

4.1.4. Validation of the Suggested Critical Buckling Moment Expression

All documented test findings on slender reinforced rectangular beams (which collapsed by buckling) are taken into account for the aim of validating the suggested formulation for M_{bcr} and comparing it to concepts found in the literature. The proposed formulation was validated by the experimental investigations undertaken by Revathi & Menon [6], Girija & Menon [8] and Sant & Bletzacker [9] and Massey [10].The published literature validated that both under-reinforced and over-reinforced beams are found to be suitable for the suggested technique.

4.1.5. Critical Buckling Moment (Generalized Formula)

Iterative procedures are used in the suggested methodology to compute M_{bcr} (Equation 8). It would be preferable to offer a more straightforward phrase that could be used in design codes. Revathi and Menon [7] provided a revised formulation that included modified formulas for effective lateral flexural rigidity (B_{eff}) and effective torsional rigidity (K_{eff}). In the current research, a similar technique is used to calculate B_{eff} and K_{eff}, with the gross cross section for flexural and torsional stiffness of UN - cracked concrete sections being as follows:

$$B_{eff} = \alpha E_c \frac{B^3 D}{12} \quad (10)$$

$$K_{eff} = \beta G_c \frac{B^3 D}{3} \quad (11)$$

In order to arrive at highly realistic estimations of B_{eff} and K_{eff}, and therefore M_{bcr}, certain modifications have often been made in the research by Girija and Menon [8]. The actual drop in depth (d_{eqv}) due to bending fracturing with respect to the major axis is accounted for the flexural stiffness coefficient (α). As d_{eqv} is acquired from $I_{eff,\,x}$, which is derived from the M–ϕ plot, the flexural rigidity coefficient (α) additionally compensated for tension hardening effect.

As demonstrated in Shebl & El-Nemr [35], it is mostly influenced by the amount of reinforcement in the tensile zone (p_t) and very slightly by the strength of concrete in compression (f_{ck}).

The following formula for obtaining α:

$$\alpha = [0.8 - 0.003 f_{ck}]\,(p_t)^{0.25} \quad (12)$$

The suggested confined formulation for α, generates results of that are remarkably similar to those obtained by the iterative method provided by Bazant and Oh [31].

Teviot & Teng's [33] solution yields the following result for the torsional stiffness co–efficient:

$$\beta = \frac{12\mu E_s {A_o}^2}{{p_o}^2 B^2 G_c\left(\frac{1}{\rho_t}+\frac{1}{\rho_{tr}}\right)} \quad (13)$$

The equation for critical buckling moment M_{bcr} may be derived by incorporating Equations 12 and 13, respectively, in Equation 9 and applying:

$$M_{bcr} = \frac{C_1 C_3}{6\, C_2 L} \frac{E_c B^3 D}{\sqrt{2(1+\upsilon_c)}} \sqrt{\alpha\beta} \quad (14)$$

where υ_c=0.15 for Poisson's ratio of concrete [7], for the present case of simply supported beam with point loads at middle third points (C_1 =1.09π, C_2=1).

The fundamental for generalized slenderness limit, which is represented as standardised moment capacity instead of compressive stress [36, 37]: $\lambda = \sqrt{M_p/M_{bcr}}$ (for beams made of steel).

The standardized slenderness limit may be calculated as:

$$\lambda = \sqrt{\frac{M_{uf}}{M_{bcr}}} \quad (15)$$

Using a common method for RC thin beams, substituting the plastic moment capacity (M_p) with the maximum flexural moment capacity (M_{uf}) (RC beams).

For λ values less than 1, the flexural mode of collapse is estimated to prevail, and for λ more than 1, the instability mode of failure is likely to occur. Though, the relationship between the two modes of failure can be predicted, in addition to decreased moment capacity, for λ = 1.

The following expression is proven by existing laboratory data and is proposed as a basis for attempting to prevent abrupt destabilization collapse in slender reinforced concrete beams. A revised formulation for minimised slenderness limit in terms of Ld./b ^{2} is also suggested based on this [7].

$$\lambda < 1.0 \quad (16)$$

4.2. Estimation of Ultimate Flexural Moment Capacity

The flexural concept developed by Singh [29]

$$\frac{M_u}{f_{ck} B D^2} = \left[0.24\xi \left(\frac{h_1}{D}\right)^2 + \left(\frac{h_2}{D}\right)^2 \left\{0.5F + \gamma\omega \left(\frac{D}{h_2}\right)\left(1 - \frac{d'}{D}\frac{D}{h_2}\right)\right\}\right] \quad (17)$$

Equation 17 may also be used to forecast the ultimate capacity of rectangular concrete sections using standard longitudinal rebars as their only main reinforcement. It's worth noting that concrete beams usually collapse due to the crushing of the concrete along their path, regardless of the amount of reinforcing given, the severe compression face. The impact of fibre characteristics, represented as fibre-index (F), and reinforcement-index (ω), on the flexural capacity (M_u) of an SFRC section is presented in this study by Singh [26]. The fibre-index (F) is a parameter for the tensile capacity of SFRC.

A high index value implies that the component has a larger capacity in flexure. According to Singh [26], the quantity of the volume percentage (V_f) and the fibre aspect ratio (ratio of length of fibre to diameter of the fibre i.e. l/d) utilised in the concrete mix rise. Concrete's compressive strength has a minor impact on the fibre-index value. As a result, SFRC beam with an increased fibre value is predicted to have a greater flexural capacity.

Both conventional RC and SFRC sections have tensile zone. Consequently, in the case of flexural SFC reinforced member with traditional tensile reinforcing bars in its tensile region, the tensile capacity of these rebars shall offer mobilization and play a vital role in adjusting the location of the NA in the segment based on the strain-value consensus at the reinforcing bar's level, with regards to the inclusion from the steel fibres existing in its tensile area.

Singh [26] conducted a study on steel fibre reinforced concrete structures and presented a flexural model to estimate the ultimate capacity of steel-fibre-reinforced rectangular sections. The volume fraction (V_f), determines the proportion of volume of steel fibres in a beam to total concrete volume of that beam. The aspect ratio of steel fibres is defined as the length of the fibre divided by its diameter. These steel fibres are understood to be dispersed randomly and displayed uniformly throughout the beam. For presenting the realistic model of a SFRC member, Singh [26], took into account the conventional reinforcement i.e. steel bars in the spanning the length of the beam with a cross-sectional area (A_{st}) at a distance d' from its bottom face as shown in Figure 16, in addition to the steel fibres. When the significant tensile stresses induced by external loads surpass the ultimate tensile strength of the material, cracking occurs in an SFRC member.

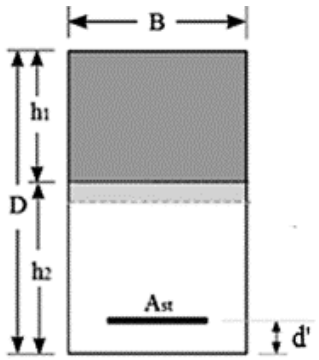

Figure 16. The cross section of the SFRC beam for the formulation presented by Singh [26]

As presented by Singh [26], the flexural capacity of SFRC members is calculated by the following expression:

$$\frac{M_u}{f_{ck}BD^2} = \left[0.24\xi\left(\frac{h_1}{D}\right)^2 + \left(\frac{h_2}{D}\right)^2\left\{0.5F + \gamma\omega\left(\frac{D}{h_2}\right)\left(1 - \frac{d'}{D}\frac{D}{h_2}\right)\right\}\right] \quad (18)$$

where (ω) is a reinforcement-index [=(A_{st}/BD) f_y/f_{ck}] and (ɣ) is a constant that specifies how much stress is mobilised in typical longitudinal tensile reinforcement bars with yield strength (f_y) under the prevailing strain state in the member. ξ has a value of unity. For every given value of the fiber-index (F), the value of the neutral-axis coefficients ($\frac{h_1}{D}, \frac{h_2}{D}$) can be computed using a series of modified expressions presented in Equation 17 for the SFRC beam sections:

$$\frac{h_1}{D} = \left(\frac{2.38F}{1+2.38F}\right) \quad (19)$$

$$\frac{h_2}{D} = \left(1 - \frac{h_1}{D}\right) \quad (20)$$

Using 19 in 20:

$$\frac{h_2}{D} = \left(\frac{1}{1+2.38F}\right) \quad (21)$$

It's worth noting that the depth of the NA i.e. the neutral axis in a steel fibrous RC beam is solely determined by the fibre-index (F), with a larger value indicating a greater strength of the material in the tension zone.

$$F = \frac{0.3\,V_f(l/d)}{\sqrt{f_{ck}}} \quad (22)$$

Using 19 and 21 in 18:

$$\frac{M_u}{f_{ck}BD^2} = \left[0.24\left(\frac{h_1}{D}\right)^2 + \left(\frac{h_2}{D}\right)^2\left\{0.5F + \gamma\omega\left(\frac{D}{h_2}\right) - \gamma\omega\left(\frac{D}{h_2}\frac{d'}{D}\frac{D}{h_2}\right)\right\}\right] \quad (23)$$

$$\frac{M_u}{f_{ck}BD^2} = \left[0.24\left(\frac{h_1}{D}\right)^2 + \left(\frac{h_2}{D}\right)^2 0.5F + \left\{\gamma\omega\left(\frac{D}{h_2}\right)\left(\frac{h_2}{D}\right)^2 - \gamma\omega\left(\frac{d'}{h_2}\frac{D}{h_2}\right)\right\}\right] \quad (24)$$

$$\frac{M_u}{f_{ck}BD^2} = \left[0.24\left(\frac{2.38F}{1+2.38F}\right)^2 + \left(\frac{1}{1+2.38F}\right)^2 0.5F + \left\{\left(\frac{\gamma\omega}{1+2.38F}\right) - \frac{\gamma\omega}{(1+2.38F)}\left(\frac{d'}{h_2}\right)\right\}\right] \quad (25)$$

Since $M_u = 0.8\,M_{uf}$ (26)

Substituting the value of M_u from Equation 26 in Equation 25:

$$\frac{M_{uf}}{f_{ck}BD^2} = \left(\frac{1}{0.8}\right)\left[0.24\left(\frac{2.38F}{1+2.38F}\right)^2 + \left(\frac{1}{1+2.38F}\right)^2 0.5F + \left\{\left(\frac{\gamma\omega}{1+2.38F}\right) - \frac{\gamma\omega}{(1+2.38F)}\left(\frac{d'}{h_2}\right)\right\}\right] \quad (27)$$

4.3. Slenderness Limits

From Equations 15 and 16:

$$\sqrt{\frac{M_{uf}}{M_{bcr}}} \leq 1.0 \quad (28)$$

Squaring Equation 28:

$$\frac{M_{uf}}{M_{bcr}} \leq 1.0 \quad (29)$$

Putting the value of M_{uf} and M_{bcr} in Equation 29:

$$\left(\frac{f_{ck}D\ 6\ C_2L\sqrt{2(1+\upsilon_c)}}{0.8C_1C_3E_cB^2\sqrt{\alpha\beta}}\right)\left[0.24\left(\frac{2.38F}{1+2.38F}\right)^2+\left(\frac{1}{1+2.38F}\right)^2 0.5F+\left\{\left(\frac{\gamma\omega}{1+2.38F}\right)-\frac{\gamma\omega}{(1+2.38F)}\left(\frac{d'}{h_2}\right)\right\}\right]\leq 1 \quad (30)$$

$$\frac{LD}{B^2}\leq\left(\frac{\sqrt{\alpha\beta}C_1C_3 0.8E_c}{\sqrt{2(1+\upsilon_c)}\,f_{ck}6C_2}\right)\left(\frac{1}{\left[0.24\left(\frac{2.38F}{1+2.38F}\right)^2+\left(\frac{1}{1+2.38F}\right)^2 0.5F+\left\{\left(\frac{\gamma\omega}{1+2.38F}\right)-\frac{\gamma\omega}{(1+2.38F)}\left(\frac{d'}{h_2}\right)\right\}\right]}\right) \quad (31)$$

where $\frac{LD}{B^2}$ represents slenderness (i.e. Limiting slenderness ratio, ƛ) according to IS 456:2000, clause 23. 3.

According to IS-456:2000, a RC simply supported beam is proportioned such that span of the beam should not exceed $\frac{250\ B^2}{d}$ [1]. Therefore for RC long beam, the lower limit of slenderness limit shall be

$$L>\frac{\mathbf{250\ B^2}}{\boldsymbol{d}} \quad (32)$$

Combining Equations 31 and 32:

$$250<\frac{LD}{B^2}\leq\left(\frac{\sqrt{\alpha\beta}C_1C_3 0.8E_c}{\sqrt{2(1+\upsilon_c)}\,f_{ck}6C_2}\right)\left(\frac{1}{\left[0.24\left(\frac{2.38F}{1+2.38F}\right)^2+\left(\frac{1}{1+2.38F}\right)^2 0.5F+\left\{\left(\frac{\gamma\omega}{1+2.38F}\right)-\frac{\gamma\omega}{(1+2.38F)}\left(\frac{d'}{h_2}\right)\right\}\right]}\right) \quad (33)$$

Equation 33 gives the final expression for slenderness limit for SFRC long beams.

Table 3. Comparison of results from experimental and theoretical formulation and the validations

S. No.	Beam Label	Moment from Experimental test results (kNm)*	Critical Buckling Moment (M_{bcr})**	Flexural Moment (M_{uf})#	To avoid instability failure Moment (M_{uf})##	Type of Failure@	Type of Failure predicted @@
1	M1S0	51.786	81.072	48.89146	Y	failure with warning (flexural cracks)	Failure with warning
2	M1S1P1	58.13938	82.175	61.86115	Y	failure with warning (flexural cracks)	Failure with warning
3	M1S2P1	58.0195	82.521	64.001	Y	failure with warning (flexural cracks)	Failure with warning
4	M2S0	62.93438	85.464	50.91609	Y	failure with warning (flexural cracks)	Failure with warning
5	M2S1P1	60.17725	85.713	77.87199	Y	failure with warning (flexural cracks)	Failure with warning
6	M2S2P1	63.41388	85.401	77.40706	Y	failure with warning (flexural cracks)	Failure with warning
7	M3S0	53.704	88.7	52.22028	Y	failure with warning (flexural cracks)	Failure with warning
8	M3S1P1	60.8965	89.1	101.0803	N	Bending	Instability Failure
9	M3S2P1	55.38225	89.4	105.6156	N	Bending	Instability Failure

* Calculation done according to simply supported beam with two point loads. ** From proposed Theoretical Formulation (kNm) [using Equation 14].

From Proposed Formulation (kNm) [using Equation 27].## From Proposed Formulation (kNm)-Mbcr>Muf-Yes(Y) or No(N) [Equation 29]

@ From Experimental test Results. @@ From Proposed formulation (Failure with warning or Instability Failure).

5. Proposals for Slenderness Ratio Limits

To prevent the sudden instability leading to failure, the design codes prescribe the limits for slenderness. Slenderness limits for long beams as proposed by Revathi and Menon [7], incorporated the effect of different variable design parameters (p_t, p_c , ρ_{tr}, f_{ck} and f_y). But this formulation showed abnormal results and to rectify the flaws in the previous study, Girija and Menon [8] further extended the concept of lateral torsional buckling of steel beams to RC long beams substituting the plastic moment capacity (M_p) of steel beams with the ultimate flexural moment capacity (M_{uf}) for RC beams.

The slenderness ratio λ can be defined as follows: $\lambda=\sqrt{M_{uf}/M_{bcr}}$ (RC beams). (18) The modified expressions for α and β proposed in the present study (Equations 12 and 13) should be incorporated in Equation 20. M_{uf} and M_{bcr} were equated to get the slenderness limit for RC long beams. But M_{uf} for SFC is different for than of RC as the effect of fibres need to be addressed. For this, the formulation by Singh [26] effectively takes into account the effect of fibres when added to the RC beam with conventional steel reinforcement. Hence, in this study the slenderness limit is suggested for SFRC long beams and the mode of failure is interpreted which is further validated by the experimental and numerical investigations. Beams with limiting slenderness ratio, ƛ values more than 1.0 are likely to fail due to instability, whilst those with ƛ values less than 1.0 will fail due to flexural tension.

The final expression for slenderness limit as stated in Equation 34 to avoid instability failure is:

$$250 < \frac{LD}{B^2} \leq \left(\frac{\sqrt{\alpha\beta}C_1C_3 0.8E_c}{\sqrt{2(1+\upsilon_c)}\, f_{ck} 6C_2}\right)\left(\frac{1}{\left|0.24\left(\frac{2.38F}{1+2.38F}\right)^2+\left(\frac{1}{1+2.38F}\right)^2 0.5F+\left\{\left(\frac{\gamma\omega}{1+2.38F}\right)-\frac{\gamma\omega}{(1+2.38F)}\left(\frac{d'}{h_2}\right)\right\}\right|}\right) \quad (34)$$

6. Conclusions

- Existing formulations for slenderness limits proposed in the literature do not predict accurately the ultimate moment capacity and mode of failure of rectangular SFRC long beams, as the limits of slenderness for RC long beams do not take into account the contribution of steel fibres, which effects the flexural moment capacity as established by 9 experimental tests conducted in the present study.
- A theoretical formulation for slenderness limits for SFRC long beams is being proposed, which has been validated against experimental tests performed in this study and the data has been presented in Table 3.
- Limiting slenderness ratio, $\lambda \leq 1.0$ suggested on the basis of avoiding sudden instability failure in long RC beams as by Revathi & Menon for long RC beams. Also, based on this, a simplified expression for limiting slenderness ratio for SFRC long beams, in terms of L_d/b^2, is proposed.
- High strength SFRC beams show instability failure in the form of bending and twisting. So the load carrying capacity in M40 grade of concrete shows better results than M55 grade, as M55 grade shows twisting and bending leading to instability failure at lower loads as compared to its load carrying capacity. Also, M40 grade shows better results as compared to M25 grade of concrete, as M25 gives a lower value of load carrying capacity as compared to M40 grade.
- The higher aspect ratio of steel fibres shows higher load carrying capacity for the M40 grade of concrete, unlike the M25 and M55 grades of concrete, which show higher load carrying capacity with lower aspect ratio for the same fibre type.
- No shear cracks were observed. All beams failed in flexure as to justify the behaviour of slender beams.
- The mode of failure as predicted based on theoretical formulation is the same as proved during experimental testing. So, the theoretical formulation predicts the behavior of the beams accurately and can hence be applied to SFRC long beams.
- A better deflection control both laterally and vertically is shown by beams with hooked end steel fibres with an aspect ratio of 77.78 as compared to the hooked end fibres with an aspect ratio of 63.63 as inferred by the load-deflection curves.
- The failure in the grade M55 of SFRC beams was due to instability because of twisting of beams and higher lateral deflection, leading to beams moving out of load assembly.

7. Declarations

7.1. Author Contributions

Conceptualization, R.K. and H.S.; investigation, R.K. and H.S.; resources, R.K. and H.S.; writing—original draft preparation, R.K. and H.S.; writing—review and editing, R.K. and H.S.; visualization, R.K. and H.S. All authors have read and agreed to the published version of the manuscript.

7.2. Data Availability Statement

The data presented in this study are available in the article.

7.3. Funding

The authors received no financial support for the research, authorship, and/or publication of this article.

7.4. Acknowledgements

The authors a very thankful to Stewols India (P) Ltd. and SRONS Engineers, Ludhiana, Punjab, India for providing Steel fibres (Hooked end aspect ratio 77.78 -STEWOLS India(P) Ltd; and Hooked end aspect ratio 63.63-SRONS Engineers, Ludhiana) used in the present study. The authors extend sincere gratefulness to the Department of Civil Engineering, Guru Nanak Dev Engineering College, Ludhiana, for giving the permission to carry out experimental research work in their Concrete Laboratory and Heavy testing Laboratory.

7.5. Conflicts of Interest

The authors declare no conflict of interest.

8. References

[1] IS 456. (2000). Plain and Reinforced Concrete-Code of Practice. Bureau of Indian Standards, New Delhi, India.

[2] BS 8110-1. (1997). Structural use of concrete. Code of practice for design and construction. British Standards Institution, London, United Kingdom.

[3] ACI 318-08. (2008). Building Code Requirements for Structural Concrete (ACI 318-08) and Commentary. American Concrete Institute (ACI), Farmington Hills, United States.

[4] EN 1992-1. (2004). Eurocode 2: Design of concrete structures. European Standard, Brussels, Belgium.

[5] AS-3600. (2001). Concrete Structures. Australian Standard, Sydney, Australia.

[6] Revathi, P., & Menon, D. (2006). Estimation of critical buckling moments in slender reinforced concrete beams. ACI Structural Journal, 103(2), 296–303. doi:10.14359/15188.

[7] Revathi, P., & Menon, D. (2007). Slenderness effects in reinforced concrete beams. ACI Structural Journal, 104(4), 412–419. doi:10.14359/18771.

[8] Girija, K., & Menon, D. (2011). Reduction in flexural strength in rectangular RC beams due to slenderness. Engineering Structures, 33(8), 2398–2406. doi:10.1016/j.engstruct.2011.04.014.

[9] Sant, J. K., & Bletzacker, R. W. (1961). Experimental Study of Lateral Stability of Reinforced Concrete Beams. ACI Journal Proceedings, 58(12). doi:10.14359/8004.

[10] Massey, C. (1967). Lateral Instablity of Reinforced Concrete Beams under Uniform Bending Moments. ACI Journal Proceedings, 64(3). doi:10.14359/7552.

[11] Chalioris, C. E., Kosmidou, P. M. K., & Karayannis, C. G. (2019). Cyclic response of steel fiber reinforced concrete slender beams: An experimental study. Materials, 12(9), 1398. doi:10.3390/ma12091398.

[12] Bafghi, M. A. B., Amini, F., Nikoo, H. S., & Sarkardeh, H. (2017). Effect of steel fiber and different environments on flexural behavior of reinforced concrete beams. Applied Sciences (Switzerland), 7(10), 1011. doi:10.3390/app7101011.

[13] Kotsovos, G., Zeris, C., & Kotsovos, M. (2007). The effect of steel fibres on the earthquake-resistant design of reinforced concrete structures. Materials and Structures, 40(2), 175-188. doi:10.1617/s11527-006-9129-5.

[14] Soutsos, M. N., Le, T. T., & Lampropoulos, A. P. (2012). Flexural performance of fibre reinforced concrete made with steel and synthetic fibres. Construction and Building Materials, 36, 704–710. doi:10.1016/j.conbuildmat.2012.06.042.

[15] Barros, J. A. O., & Figueiras, J. A. (1999). Flexural Behavior of SFRC: Testing and Modeling. Journal of Materials in Civil Engineering, 11(4), 331–339. doi:10.1061/(asce)0899-1561(1999)11:4(331).

[16] Campione, G., & Letizia Mangiavillano, M. (2008). Fibrous reinforced concrete beams in flexure: Experimental investigation, analytical modelling and design considerations. Engineering Structures, 30(11), 2970–2980. doi:10.1016/j.engstruct.2008.04.019.

[17] Chalioris, C. E., & Panagiotopoulos, T. A. (2018). Flexural analysis of steel fibre-reinforced concrete members. Computers and Concrete, 22(1), 11–25. doi:10.12989/cac.2018.22.1.011.

[18] Kwak, Y. K., Eberhard, M. O., Kim, W. S., & Kim, J. (2002). Shear strength of steel fiber-reinforced concrete beams without stirrups. ACI Structural journal, 99(4), 530-538. doi:10.14359/12122.

[19] Sharma, A. K. (1986). Shear Strength of Steel Fiber Reinforced Concrete Beams. ACI Journal Proceedings, 83(4). doi:10.14359/10559.

[20] Li, V. C., Ward, R., & Hamza, A. M. (1992). Steel and synthetic fibers as shear reinforcement. ACI Materials Journal, 89(5), 499–508. doi:10.14359/1822.

[21] Narayanan, R., & Darwish, I. Y. S. (1988). Fiber Concrete Deep Beams in Shear. ACI Structural Journal, 85(2), 141–149. doi:10.14359/2698.

[22] Khuntia, M., Stojadinovic, B., & Goel, S. C. (1999). Shear strength of normal and high-strength fiber reinforced concrete beams without stirrups. ACI Structural Journal, 96(2), 282–289. doi:10.14359/620.

[23] Slater, E., Moni, M., & Alam, M. S. (2012). Predicting the shear strength of steel fiber reinforced concrete beams. Construction and Building Materials, 26(1), 423–436. doi:10.1016/j.conbuildmat.2011.06.042.

[24] Ashour, S. A., Hasanain, G. S., & Wafa, F. F. (1992). Shear Behaviour of High-Strength Fiber-Reinforced Concrete Beams. ACI Structural Journal, 89(2). doi:10.14359/2946.

[25] Shin, S. W., Oh, J. G., & Ghosh, S. K. (1994). Shear behavior of laboratory-sized high-strength concrete beams reinforced with bars and steel fibers. SP-142: Fiber Reinforced Concrete Developments and Innovations, 142, 181-200. doi:10.14359/3917.

[26] Singh, H. (2017). Steel Fiber Reinforced Concrete Behavior, Modelling and Design. Springer Transactions in Civil and Environmental Engineering, Springer, Singapore. doi:10.1007/978-981-10-2507-5.

[27] Hansell, W., & Winter, G. (1959). Lateral Stability of Reinforced Concrete Beams. ACI Journal Proceedings, 56(9), 193–215. doi:10.14359/8091.

[28] Chen, W. F., & Lui, E. M. (1987). Structural Stability Theory and Implementation. Prentice Hall, Hoboken, United States.

[29] Bleich, F. (1952). Buckling strength of metal structures. McGraw-Hill book Company, New York City, United States.

[30] Timoshenko, S. P., & Gere, J. M. (1961). Theory of Elastic Stability. McGraw-Hill book Company, New York City, United States.

[31] Bazant, Z. P., & Oh, B. H. (1984). Deformation of Progressively Cracking Reinforced Concrete Beams. Journal of the American Concrete Institute, 81(3), 268–278. doi:10.1016/0010-4485(84)90120-9.

[32] Branson, D. E. (1968). Design Procedures for Computing Deflections. ACI Journal Proceedings, 65(9). doi:10.14359/7508.

[33] Tavio, & Teng, S. (2004). Effective Torsional Rigidity of Reinforced Concrete Members. ACI Structural Journal, 101(2), 252–260. doi:10.14359/13023.

[34] Hsu, T. T. C. (1973). Post-Cracking Torsional Rigidity of Reinforced Concrete Sections. ACI Journal Proceedings, 70(5). doi:10.14359/11218.

[35] Shebl, H., & El-Nemr, A. (2021). Moment Redistribution of Shear-Critical GFRP Reinforced Continuously Supported Slender Beams. Civil Engineering Journal, 7, 13-31. doi:10.28991/cej-sp2021-07-02.

[36] Simões, T., Octávio, C., Valença, J., Costa, H., …., & Júlio, E. (2017). Influence of concrete strength and steel fibre geometry on the fibre/matrix interface. Composites Part B: Engineering, 122, 156–164. doi:10.1016/j.compositesb.2017.04.010.

[37] Kirby, P. A., & Nethercot, D. A. (1979). Design for structural stability. Constrado Monographs. John Wiley & Sons, Hoboken, United States.